J. Phys.: Condens. Matter **8** (1996) A19–A37. Printed in the UK

Cluster formation in water-in-oil microemulsions at percolation: evaluation of the electrical properties

F Bordi†, C Cametti‡, J Rouch§, F Sciortino‡ and P Tartaglia‡

† Sezione di Fisica Medica, Dipartimento di Medicina Interna, Università di Roma Tor Vergata, 00175 Roma, Italy, and Istituto Nazionale di Fisica della Materia, Unità di Roma La Sapienza, Roma, Italy

‡ Dipartimento di Fisica and Istituto Nazionale di Fisica della Materia, Università di Roma La Sapienza, Piazzale Aldo Moro 2, Roma, Italy

§ Centre de Physique Moléculaire Optique et Hertzienne (URA 283 du CNRS), Université Bordeaux I, 351 Cours de la Libération, 3405 Talence, France

Received 19 December 1995, in final form 23 April 1996

Abstract. We study water-in-oil microemulsion systems in the droplet phase and in the vicinity of a percolation transition in the non-percolating region. We focus on the electrical conductivity and permittivity, quantities that show large variations when approaching the percolation threshold. The accepted model for the interpretation of the increasing conductivity—very large compared to that of the bathing oil phase—is related to clustering of the microemulsion droplets and migration of charges within the aggregates. Power laws have been used to interpret the behaviour of the static dielectric properties and scaling functions proposed for the frequency-dependent conductivity and permittivity. We review some relevant experiments in this field and the proposed interpretations, and formulate a phenomenological model of conduction. It is based on the physical picture of cluster formation due to attractive interactions among the constituent water droplets, anomalous diffusion in the bulk of fractal aggregates and polydispersity of the clusters. The model gives quantitative expressions for both conductivity and permittivity over the entire frequency range of the percolative relaxation phenomena, including the static behaviour. A closed expression is derived for the scaling function of a scaling variable which involves frequency, the cut-off cluster size and the parameters of the bulk components. The results are also expressed in the time domain in terms of the polarization time correlation function. The latter exhibits a rather interesting behaviour, since it gradually evolves from an exponential decay to a power-law decay and to a stretched exponential as time increases. The time-scales of the different stages are obtained from the typical decay times of the single droplet and the largest cluster. We have analysed many different sets of data obtained for different microemulsion systems as functions of the composition of the dispersed phase, the temperature and the frequency of the applied field, with a very good agreement with the model in all cases.

1. Introduction

In recent years complex liquid systems have become a rather rapidly developing field of research, the aim being the understanding of the behaviour of supramolecular aggregates and, at the same time, the use of them as model systems for the study of important statistical mechanics phenomena, such as structure formation, critical point anomalies and percolative transitions. In this paper we will be mainly interested in a particular type of supramolecular liquid which is an excellent model system for the study of percolation, i.e. microemulsions. In this case the system is made up of water droplets immersed in an oil bath where the two immiscible components are separated by a surfactant layer. These surfactant-coated

0953-8984/96/SA0019+19$19.50

droplets interact via a short-ranged attractive potential and form a spanning cluster made of water droplets for certain values of temperature and composition. We define as the percolation line the locus of points that separates the plane of the thermodynamic variables into a region where an infinite cluster is not present and one in which it appears. The existence of a percolative phenomenon for the droplets has been demonstrated by a number of experiments [1–8]. The crossing of the percolation line is accompanied by a large increase of the system electrical conductivity. A small but finite conductivity exists in the system even below the percolation threshold, related to the finite small conductivity of the oil. We will study in particular the mechanism of conduction of the highly conducting water droplets in the poorly conducting medium below the percolation threshold.

The problem of conductivity in percolating systems has been treated in the framework of lattice models, the sites being randomly connected by circuit elements [9]. The general theoretical result for the conductivity and the permittivity, on approaching the percolation transition, is a scaling expression, valid for both the static and the dynamic case, and the identification of the relevant indices for the corresponding power laws. A physical interpretation [10–13] of this phenomenon in microemulsions has been given in terms of anomalous diffusion of charge carriers, originating from the polar heads of the surfactant, on the droplet fractal aggregates produced by the interdroplet potential.

An explicit expression for the scaling function for electrical conductivity and permittivity, that can be compared with the experimental results, has never been derived, and it is the main result of the present work. We will apply an effective-medium theory in order to extract the correct dependence on the microemulsion components together with an *ansatz* for the relaxation amplitude and decay time of the polarization of a fractal cluster, obtained from considerations on the anomalous diffusive motion of charges in the aggregates. The final step is obtained taking into account the polydispersity of the microemulsion droplets. The expressions that we obtained for the conductivity and the dielectric constant are in very good agreement with the measured data for different systems and various experimental conditions.

The paper is organized as follows. Section 2 will briefly summarize the experimental results concerning both the conductivity and the permittivity of the microemulsions. We will consider both the static behaviour, which led to the determination of the critical indices relevant to this type of percolation, and the dynamic behaviour which shows a marked relaxation phenomenon in the region from 1 to 10 MHz. Section 3 will report the detailed calculation of the complex conductivity of the system. The scaling properties of the complex conductivity are reviewed in section 4 where a complex scaling function of a complex scaling variable is introduced in order to take into account the two measurable physical quantities, conductivity and permittivity, and their dependence on the parameters of the materials and the thermodynamic state of the system. Section 5 is devoted to the reformulation of the results in the time domain, where a definite succession of behaviours, exponential, power-law and stretched exponential, is clearly evident for the time correlation function of the polarization of the microemulsion system. In section 6 we compare our analytical results with a large variety of measurements. We draw our final conclusions in section 7.

2. Experimental results on conductivity and permittivity

The measurements of conductivity and permittivity of self-assembled complex liquids are relatively recent. The overall picture that emerges from the experimental data consistently indicates that the anomalous electric behaviour is closely related to the percolative phenomena. All of these studies have in common the parametrization of the static behaviour

of the conductivity of the microemulsions in terms of a characteristic power-law behaviour, as a function of the distance from a percolation point and with associated percolation indices. For the conductivity σ below percolation, when approaching the threshold in temperature at constant composition ($T < T_p$),

$$\sigma = A(T_p - T)^{-s'} \tag{1}$$

where A is the divergence amplitude and s' the index. Above percolation ($T > T_p$)

$$\sigma = B(T - T_p)^t \tag{2}$$

with amplitude B and index t. These power laws are similarly valid when approaching the percolation line in composition at constant temperature. In both cases the diverging behaviour when approaching percolation from below, and the vanishing behaviour when approaching from above are valid when close to the percolation line, but not in a narrow region around it, where the conductivity reaches a finite value. As far as the static permittivity is concerned, there is an apparent divergence from both sides of the percolation threshold. The indices are difficult to extract, but are close to s'.

The frequency-dependent conductivity measurements are parametrized as power laws in frequency with an exponent denoted as u, the analogous permittivity data with the exponent $u - 1$. In all cases the path of approach to the percolation threshold is a function of temperature at constant composition or a function of composition at constant temperature.

The phenomenon of percolation in microemulsions was initially studied by Lagües *et al* [1] in the quaternary water-in-oil system water–cyclohexane–1-pentanol–sodium dodecyl-sulphate. One of the first measurements which showed in a rather clear way the existence of a maximum of the static permittivity in a microemulsion system made of water, AOT (sodium diethyl-hexyl-sulphosuccinate) and iso-octane is due to van Dijk [2], who also measured the dynamic index $u = 0.62 \pm 0.02$. Bhattacharya *et al* [3] measured similarly the static dielectric characteristics of a water–AOT–decane (WAD from now on) system and found an anomalously large increase of the conductivity and the dielectric constant on approaching percolation. They were able to measure the indices $s' = 1.17 \pm 0.05$, $t = 1.68 \pm 0.05$ and $u = 0.63 \pm 0.04$, and to test at the same time the validity of the dynamical theory of percolation in microemulsions [10, 11]. A rather wide study on these systems was also performed by the group of Boned and Peyrelasse (see [4]) who examined various three- and four-component systems. Clarkson (see [5]) also carefully measured the dielectric properties of a multicomponent microemulsion composed of toluene, brine, sodium dodecyl-sulphate and butanol, and tried to interpret them in terms of classical models of interfacial polarization [14]. A rather detailed study on the WAD system as a function of temperature over a wide range of composition in static conditions was performed by our group [6], with the results $s' = 1.2 \pm 0.1$ and $t = 1.9 \pm 0.1$. We also measured dielectric relaxation over a rather large frequency range [22], and obtained $u = 0.62 \pm 0.10$. More recently Ponton and Bose (see [7]) measured the complex permittivity of a water–AOT–iso-octane system and confirmed the validity of the dynamic percolation model. Their measured power-law indices are $s' = 1.35$, $t = 1.80$ and $u = 0.61$.

3. The independent-clusters approach

The calculation of the complex conductivity that we perform in this section is based on the possibility of selecting clusters that can be considered independent of one another. We start by considering the complex conductivity due to a single aggregate. At this stage we take into account both (i) the correct dependence of the system complex conductivity from

the electric parameters of the microemulsion components and (ii) the mechanism that, even below percolation, gives rise to a finite conductivity for the entire system. The first step is accomplished using an effective-medium approximation; the second one is based on the physical mechanism of anomalous diffusion in the bulk of a fractal cluster, which grows through the successive aggregation of microemulsion droplets. The result is a conductivity for the single cluster which has the typical form of a single-relaxation phenomenon, where the relaxational amplitude and time have the power-law dependence on cluster size typical of systems with scaling properties. The final step consists in using the appropriate cluster size distribution to account for the polydispersity of the system close to percolation.

Before starting the calculation, it is important to note that we are considering clusters formed by nearest-neighbour droplets. We have to stress that the definition of percolation depends in an essential way on the type of cluster that we consider, which in turn depends on the physical quantity that is experimentally observed. For example, for light scattering experiments [15], it has been recently shown by Coniglio and Klein [16], that in discrete lattice models the independent clusters which lead to a correct definition of the space correlation function are not the ones defined by the criterion of being nearest neighbours. The proper procedure of definition of percolating clusters amounts to a type of dilution of the bonds connecting the sites. Coniglio and Klein give an exact rule for partitioning sites in clusters in such a way that the resulting independent clusters are the ones that are effectively seen through light scattering.

3.1. The effective-medium approximation

Let us consider a matrix of oil, characterized by the conductivity σ_A and dielectric constant ϵ_A, containing a single spherical droplet of volume v, the electrical parameters of which are σ_B and ϵ_B. A uniform external frequency-dependent electric field is applied. The resulting electric field potential can be easily derived in the far-field approximation by solving the appropriate Laplace equation. The result is easily generalized to the case of many independent particles and interpreted as being generated by a single homogeneous system of total volume V, with the electrical characteristics that generate the same electric field at large distances. This procedure is referred to as the effective-medium approximation (EMA) [17, 18]. We apply this method to the calculation of the conductivity and the permittivity of a cluster containing k droplets, σ_k and ϵ_k respectively. We introduce the complex conductivity of the cluster $\widetilde{\sigma}_k = \sigma_k + \mathrm{i}\omega\epsilon_k$ which is expressed in terms of the complex conductivities of the medium $\widetilde{\sigma}_A = \sigma_A + \mathrm{i}\omega\epsilon_A$ and of the inclusions $\widetilde{\sigma}_B = \sigma_B + \mathrm{i}\omega\epsilon_B$:

$$\widetilde{\sigma}_k = \widetilde{\sigma}_A \frac{A_k\widetilde{\sigma}_B + 2\widetilde{\sigma}_A}{\widetilde{\sigma}_B + B_k\widetilde{\sigma}_A} \tag{3}$$

where A_k and B_k are given by [18]

$$A_k = \frac{1+2f_k}{1-f_k} \qquad B_k = \frac{2+f_k}{1-f_k} \tag{4}$$

and $f_k = kv/V$ is the inclusions volume fraction. Note that A_k and B_k do not depend on the electrical properties of the materials. Equation (3) can be written in an equivalent way in terms of the complex permittivity $\widetilde{\epsilon}_k(\omega)$ using the relations

$$\widetilde{\sigma}_k(\omega) = \mathrm{i}\omega\widetilde{\epsilon}_k(\omega) = \sigma_{k0} + \mathrm{i}\omega\epsilon_{k\infty}\,[1 + \widetilde{\chi}_k(\omega)] \tag{5}$$

where $\widetilde{\chi}_k(\omega)$ is the dielectric susceptibility, σ_{k0} the low-frequency conductivity and $\epsilon_{k\infty}$ the high-frequency permittivity. From (3) and (5) we can derive σ_{k0} and $\epsilon_{k\infty}$:

$$\sigma_{k0} = \sigma_A \frac{A_k\sigma_B + 2\sigma_A}{\sigma_B + B_k\sigma_A} \qquad \epsilon_{k\infty} = \epsilon_A \frac{A_k\epsilon_B + 2\epsilon_A}{\epsilon_B + B_k\epsilon_A}. \tag{6}$$

The susceptibility $\widetilde{\chi}_k(\omega)$ is given by [18]

$$\epsilon_{k\infty}\widetilde{\chi}_k(\omega) = \epsilon_A \frac{\Delta_k}{1 + \mathrm{i}\omega\tau_k}. \tag{7}$$

It has the typical form of a single-relaxation process with amplitude Δ_k and relaxation time τ_k given by

$$\Delta_k = \frac{(A_k B_k - 2)(\sigma_B\epsilon_A - \sigma_A\epsilon_B)^2}{\epsilon_A(\sigma_B + B_k\sigma_A)^2(\epsilon_B + B_k\epsilon_A)} \qquad \tau_k = \frac{\epsilon_B + B_k\epsilon_A}{\sigma_B + B_k\sigma_A}. \tag{8}$$

Note that while the parameters A_k and B_k are independent of the conductivity and dielectric constant of the components, the two quantities Δ_k and τ_k depend on the material's electrical parameters.

As we mentioned earlier, in general the EMA is applicable when the particles that constitute the system are weakly interacting and therefore not in the case of a cluster where the droplets are strictly bound. For this reason we assume that the EMA expressions are still valid, but we do not specify the coefficients A_k and B_k as in (4). We use the physical mechanism of conduction below the percolation threshold in order to derive an expression for the coefficients. Using the EMA expressions (3), but with a scaling assumption for A_k and B_k, we expect to retain the correct dependence of the complex conductivity of the system on the electrical parameters of the two components as discussed above.

3.2. The resistor–capacitor (RC) case

It is well known that, when considering dielectric properties, the systems that we study can also be considered as a set of electric circuit elements connecting lattice sites. If we model the system only as resistive or capacitive bonds then this corresponds in our case to discarding the oil conductivity and the droplet permittivity in the appropriate frequency range according to

$$\omega_A = \frac{\sigma_A}{\epsilon_A} \ll \omega \qquad \omega \ll \omega_B = \frac{\sigma_B}{\epsilon_B} \tag{9}$$

where we introduced the two frequencies

$$\omega_A = \frac{\sigma_A}{\epsilon_A} \qquad \omega_B = \frac{\sigma_B}{\epsilon_B}. \tag{10}$$

We will call the approximation of conducting clusters in an ideal non-conducting medium the *RC* model. In the case of the WAD system [6] we estimate $\sigma_A \approx 10^{-6}\ \Omega^{-1}\ \mathrm{m}^{-1}$, $\epsilon_A \approx 2\epsilon_0$ and $\sigma_B \approx 10^{-2}\ \Omega^{-1}\ \mathrm{m}^{-1}$, $\epsilon_B \approx 10^2\epsilon_0$, with ϵ_0 the vacuum permittivity, and therefore we expect for the parameters $\omega_A \approx 100$ kHz and $\omega_B \approx 1$ GHz. In the frequency range $\omega_A \ll \omega \ll \omega_B$ the WAD system is close to the *RC* case. The amplitude and the relaxation time for a relaxing cluster of k particles become in the *RC* case

$$\Delta_k^{RC} = A_k - \frac{2}{B_k} \qquad \tau_k^{RC} = \frac{\epsilon_A B_k}{\sigma_B}. \tag{11}$$

3.3. Cluster relaxation

The two parameters A_k and B_k must now be determined as a function of the number of particles k in a k-cluster. In order to do this, we must refer to a physical mechanism of percolation in microemulsions below the percolation threshold. This mechanism, introduced some time ago by Lagües *et al* (see [10]) is known as *stirred percolation* and was studied later on in a more detailed way by Grest *et al* [11] and named *dynamic percolation*. The

main idea is that once the microemulsion droplets aggregate to form clusters, the charge carriers are capable of moving in the cluster, thus giving rise to conduction. The motion of the charges in the aggregate is essentially anomalous diffusion on a fractal cluster. The diffusive motion of the charge carriers in turn generates dipole moment fluctuations. The complex frequency-dependent susceptibility of a k-cluster is in general related to the Laplace transform time derivative of the total dipole moment fluctuation ($\delta\mu$) time correlation function $\langle\delta\mu(t)\delta\mu(0)\rangle$.

We start in the RC limit and, on the basis of (8), relate the relaxational amplitude Δ_k^{RC} to the static dipole moment correlation function $\langle(\delta\mu(0))^2\rangle$ and the relaxation time τ_k^{RC} to its exponential decay constant. Δ_k is related to the product of the mean square charge fluctuations, and proportional to the cluster size k, and the radius of gyration squared R_k^2, where $R_k \sim k^{1/D}$ and D is the fractal dimension of the cluster. Consequently Δ_k^{RC} will be proportional as follows [19]:

$$\Delta_k^{RC} \approx k R_k^2. \tag{12}$$

If the clusters were compact objects τ_k^{RC} would be proportional to R_k^2 since the charge carriers perform diffusive motion in the clusters. Since the motion is instead on a fractal aggregate, it is governed by anomalous diffusion and τ_k^{RC} will be related to the radius of gyration through a power which takes into account the anomaly, i.e. the ratio $D/\tilde{d}$:

$$\tau_k^{RC} \approx (R_k^2)^{D/\tilde{d}} \tag{13}$$

where $\tilde{d}$ is the spectral exponent. This approximation gives the following simple expressions for A_k and B_k:

$$A_k = \left(A_1 - \frac{2}{B_1}\right)k^{1+2/D} + \frac{2}{B_k} \qquad B_k = B_1 k^{2/\tilde{d}}. \tag{14}$$

At this point, if we take into account the fact that both of these constants are independent of the material's electrical parameters, then the results given by the preceding equations, derived in the RC case, are valid in general. The previous equation introduces the two parameters A_1 and B_1 that can be related to microscopic physical quantities using (8) in the case of a monomer, i.e. when $k = 1$. Therefore A_1 and B_1 are related to the monomer amplitude Δ_1 and relaxation time τ_1 according to

$$A_1 - \frac{2}{B_1} = \Delta_1 \frac{(\omega_B - \omega_A)\tau_1}{(\omega_B\tau_1 - 1)(1 - \omega_A\tau_1)^2} \qquad B_1 = \frac{\epsilon_B}{\epsilon_A}\left(\frac{\omega_B\tau_1 - 1}{1 - \omega_A\tau_1}\right). \tag{15}$$

Figure 1 shows the k-dependence of Δ_k and τ_k:

$$\Delta_k = \frac{\Delta_1\tau_1 k^{1+2/D+2/\tilde{d}}(\omega_B - \omega_A)^3}{[\omega_B(1 - \omega_A\tau_1) + \omega_A(\omega_B\tau_1 - 1)k^{2/\tilde{d}}]^2[(1 - \omega_A\tau_1) + (\omega_B\tau_1 - 1)k^{2/\tilde{d}}]} \tag{16}$$

$$\tau_k = \frac{(1 - \omega_A\tau_1) + (\omega_B\tau_1 - 1)k^{2/\tilde{d}}}{\omega_B(1 - \omega_A\tau_1) + \omega_A(\omega_B\tau_1 - 1)k^{2/\tilde{d}}} \tag{17}$$

corresponding to the A_k- and B_k-expressions given in (14) and (15) for typical values of the parameters. We show also the corresponding curves for the pure RC case, to highlight the deviations from the power-law behaviour at small and high cluster sizes. Note that the shortest time-scale is given by the minimum value of the cluster relaxation time τ_1, while the longest time-scale is $\tau_\infty = \omega_A^{-1}$.

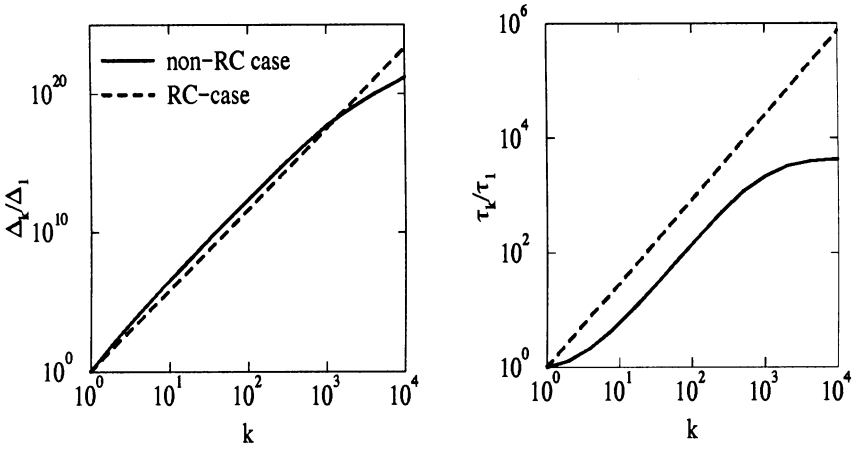

Figure 1. Δ_k/Δ_1 and τ_k/τ_1 for the *RC* case (dashed lines) and for one non-*RC* case ($\omega_A = 0.5$ MHz, $\omega_B = 2.8$ GHz, $\tau_1 = 0.42$ ns, full lines). Note that in the non-*RC* case the power-law behaviour of τ_k and Δ_k is observed only for a limited range of k-values.

We conclude this section by writing out the final expression that we have obtained for the complex conductivity of an isolated cluster:

$$\widetilde{\sigma}_k = \widetilde{\sigma}_A \frac{\widetilde{\sigma}_B[(A_1 - 2/B_1)k^{1+2/D} + (2/B_1)k^{-2/\tilde{d}}] + 2\widetilde{\sigma}_A}{\widetilde{\sigma}_B + \widetilde{\sigma}_A B_1 k^{2/\tilde{d}}}. \tag{18}$$

The preceding equation was derived using the EMA, in order to get the dependence on the material's parameters, and the dynamic model for conduction below percolation, in order to get the dependence on the number of monomers in a cluster.

3.4. Polydispersity

It is well known that close to the threshold in random-bond percolation the number of clusters of size k is given by a typical scaling expression [20]

$$c(k) = \frac{Nk^{-\tau}\mathrm{e}^{-k/k_c}}{k_c^{2-\tau}\Gamma(2-\tau, k_c^{-1})} \tag{19}$$

characterized by a power-law behaviour with index τ and a cut-off cluster size k_c which diverges as the system approaches the percolation threshold.

$$\Gamma(a, z) = \int_z^\infty \mathrm{d}x\ \mathrm{e}^{-x}x^{a-1}$$

is the incomplete Gamma function and N is the initial number of monomers [21]. The normalization of $c(k)$ is such that

$$\int_1^\infty \mathrm{d}k\ kc(k) = N. \tag{20}$$

In the limit when k_c is large, the following approximation holds:

$$c(k) \approx N(\tau - 2)k^{-\tau}\mathrm{e}^{-k/k_c}. \tag{21}$$

We assume that a distribution similar to the one in (19) describes our case. We calculate $\widetilde{\sigma}$ as a sum of independent contributions $\widetilde{\sigma}_k$ weighted with the distribution given by (19)

$$\widetilde{\sigma}(\omega) = \int_1^\infty \mathrm{d}k\ c(k)\widetilde{\sigma}_A \frac{A_k\widetilde{\sigma}_B + 2\widetilde{\sigma}_A}{\widetilde{\sigma}_B + B_k\widetilde{\sigma}_A} \tag{22}$$

where A_k and B_k are given by (14). In terms of the cluster relaxation process we can write

$$\widetilde{\sigma}(\omega) = \int_1^\infty \mathrm{d}k\ c(k)\left(\sigma_{k0} + \mathrm{i}\omega\epsilon_{k\infty} + \mathrm{i}\omega\frac{\Delta_k}{1+\mathrm{i}\omega\tau_k}\right) \tag{23}$$

where σ_{k0} and $\epsilon_{k\infty}$ are given in (6).

In order to evaluate the indices that we have introduced so far in terms of a limited set of power-law exponents, we recall the definition of ν as the index for the divergence of connectivity in bond percolation, when the bond probability approaches the threshold. In three dimensions $\nu = 0.88$, $D = 2.52$, $\tilde{d} = 1.36$ are the accepted values [20]. We can express the conductivity exponents s', t and u in terms of the set ν, D and $\tilde{d}$ in d space dimensions [20]:

$$s' = \left(1 - \frac{d-2}{D}\right)D\nu \tag{24}$$

$$t = \frac{2D\nu}{\tilde{d}} - s' = \left(\frac{2}{\tilde{d}} + \frac{d-2}{D} - 1\right)D\nu \tag{25}$$

$$u = \frac{t}{s'+t} = \left(\frac{2}{\tilde{d}} + \frac{d-2}{D} - 1\right)\frac{\tilde{d}}{2} \tag{26}$$

while the cluster size distribution exponent τ obeys the relation

$$\tau = 1 + \frac{d}{D}. \tag{27}$$

4. Scaling properties of the complex conductivity

In order to get an explicit expression for the complex conductivity, we substitute (14) into (22). Since the system is close to the percolation threshold, we keep only terms to lowest order in k_c^{-1} to get

$$\widetilde{\sigma}(\omega) = \Sigma_u\widetilde{\sigma}_B B_1\tilde{h}\int_1^\infty \mathrm{d}k\ \frac{\mathrm{e}^{-k/k_c}k^{-1/D}}{1 + B_1\tilde{h}k^{2/\tilde{d}}} \tag{28}$$

where $\tilde{h}$ is the ratio of the complex conductivities of the two components:

$$\tilde{h} = \frac{\tilde{\sigma}_A}{\tilde{\sigma}_B} \tag{29}$$

and the adimensional conductivity scale, Σ_u, is given by

$$\Sigma_u = N(\tau-2)\left(A_1 - \frac{2}{B_1}\right)\frac{1}{B_1}. \tag{30}$$

Using (15), Σ_u can also be written as

$$\Sigma_u = N(\tau-2)\Delta_1\frac{\epsilon_A}{\epsilon_B}\frac{(1-\omega_A\tau_1)(\omega_B-\omega_A)\tau_1}{(\omega_B\tau_1-1)^2}. \tag{31}$$

Changing the variable in the integral we get

$$\widetilde{\sigma}(\omega) = \Sigma_u\widetilde{\sigma}_B k_c^{-t/D\nu}\widetilde{\Phi}_{k_c}(\zeta) \tag{32}$$

where $\widetilde{\Phi}_{k_c}(\zeta)$ is defined by

$$\widetilde{\Phi}_{k_c}(\zeta) = \zeta \int_{k_c^{-1}}^{\infty} \mathrm{d}z \; \frac{\mathrm{e}^{-z} z^{-1/D}}{1 + \zeta z^{2/\tilde{d}}} \tag{33}$$

and is a complex function of the real variable k_c and the complex variable ζ:

$$\zeta = B_1 \tilde{h} k_c^{2/\tilde{d}} = \frac{\omega_B \tau_1 - 1}{1 - \omega_A \tau_1} \frac{\omega_A + \mathrm{i}\omega}{\omega_B + \mathrm{i}\omega} k_c^{2/\tilde{d}}. \tag{34}$$

While ζ has the typical properties of a scaling variable, the function $\widetilde{\Phi}_{k_c}(\zeta)$ is not a scaling function because of the residual dependence on k_c given by the lower limit of integration in (33). ζ involves four parameters, namely the cut-off cluster size k_c which measures the distance from the percolation threshold, the monomer relaxation time τ_1 and the two frequencies ω_A and ω_B referring to the electrical characteristics of the dispersed phase and the medium respectively. In the *RC* limit $\omega_A = 0$ and $\omega_B = \infty$, so

$$\zeta = \mathrm{i}\omega\tau_1 k_c^{2/\tilde{d}}.$$

The complex conductivity that we derived depends on five parameters, the ones that we listed above, i.e. ω_A, ω_B, τ_1, k_c, and the conductivity scale Σ_u. The first four parameters are necessary to define the two-component system, and can be, in an equivalent way, expressed in terms of σ_A, σ_B, ϵ_A and ϵ_B, the four material parameters of the two-component system. The parameter k_c is a physical quantity extracted from the experimental data by the procedure of fitting to the frequency dependence of the conductivity and permittivity. Note that any theory would need essentially the same number of parameters which are the minimal set for describing the relaxation. Even the use of a simple interpolation formula like Cole–Davidson's needs five parameters, namely the zero-frequency conductivity and the high-frequency permittivity, the relaxation amplitude and time, and the characteristic Cole–Davidson exponent. Moreover these quantities would have a dependence on the distance from percolation, which is obtained in our case by means of k_c.

4.1. Properties of the function $\widetilde{\Phi}_{k_c}(\zeta)$

We will now study in a more detailed fashion the properties of the function $\widetilde{\Phi}_{k_c}(\zeta)$. A series expansion around $\zeta = 0$ gives

$$\widetilde{\Phi}_{k_c}(\zeta) \approx \Gamma\left(1 - \frac{1}{D}, \frac{1}{k_c}\right)\zeta - \Gamma\left(1 - \frac{1}{D} + \frac{2}{\tilde{d}}, \frac{1}{k_c}\right)\zeta^2 + \cdots. \tag{35}$$

For large values of k_c the incomplete Gamma functions tend to the usual Gamma functions and (35) gives, to lowest order,

$$\widetilde{\sigma}(\omega) \approx \Sigma_u \tilde{\sigma}_B \Gamma\left(1 - \frac{1}{D}\right) B_1 \tilde{h} k_c^{s'/D\nu}. \tag{36}$$

In the static limit $\sigma_0 = \lim_{\omega\to 0}\tilde{\sigma}(\omega)$ and $\epsilon_0 = \lim_{\omega\to 0}\tilde{\epsilon}(\omega)$

$$\sigma_0 \approx \Sigma_u \sigma_A \Gamma\left(1 - \frac{1}{D}\right) B_1 k_c^{s'/D\nu} = \omega_A \epsilon_0 \tag{37}$$

and thus the expected power-law behaviour for the static conductivity and permittivity is recovered. Figure 2 shows the k_c-dependence of σ_0 and ϵ_0 for typical values of the parameters and for the pure *RC* case. It also shows the longest relaxation time in the system, τ_c. Note that a power-law region is observed in the three quantities at intermediate k_c-values, with the exponents $s'/D\nu$ for σ_0 and ϵ_0 and $(t + s')/D\nu = 2/\tilde{d}$ for τ_c. The deviations from the *RC* case produce finite values for the various quantities at large k_c.

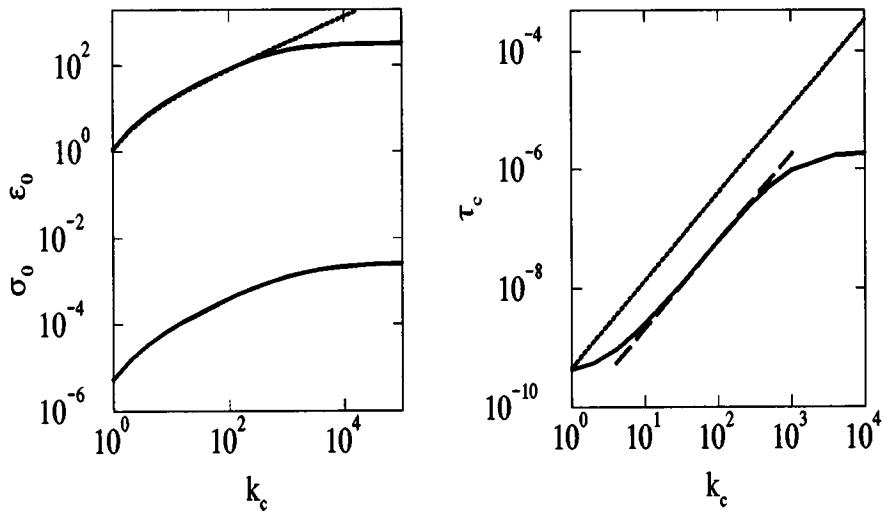

Figure 2. The k_c-dependence of σ_0, ϵ_0 and τ_c for the same parameters as in figure 1 (full lines). The dashed line shows the corresponding case for *RC* systems. Note that in the *RC* case σ_0 is zero below percolation.

The asymptotic behaviour of $\widetilde{\Phi}_{k_c}(\zeta)$ for large values of ζ can be easily obtained from (33) when $|\zeta| \gg k_c^{2/\tilde{d}}$. In this case the approximation is

$$\widetilde{\Phi}_{k_c}(\zeta) \approx \int_{k_c^{-1}}^{\infty} \mathrm{d}z\ \mathrm{e}^{-z} z^{-1/D-2/\tilde{d}} = \Gamma\left(-\frac{t}{D\nu}, \frac{1}{k_c}\right) \approx k_c^{t/D\nu} \tag{38}$$

where we have used the properties of the incomplete Gamma function for small values of the second argument. Therefore for large values of $|\zeta|$ the function $\widetilde{\Phi}_{k_c}(\zeta)$ becomes constant. For large values of $|\zeta|$, but $|\zeta| \ll k_c^{2/\tilde{d}}$, we transform the integral of (33) as

$$\widetilde{\Phi}_{k_c}(\zeta) = \frac{\tilde{d}}{2}\zeta^u \int_{\zeta/k_c^{-2/\tilde{d}}}^{\infty} \mathrm{d}\lambda\ \exp\left[-\left(\frac{\lambda}{\zeta}\right)^{\tilde{d}/2}\right] \frac{\lambda^{-u}}{1+\lambda} \tag{39}$$

which for large k_c reduces to

$$\widetilde{\Phi}_{k_c}(\zeta) \approx \frac{\tilde{d}}{2}\frac{\pi}{\sin(\pi u)}\zeta^u \tag{40}$$

and gives a power-law behaviour characterized by the exponent u. If we call $|\zeta_c|$ the crossover point between the power-law behaviour and the constant value of $\widetilde{\Phi}_{k_c}(\zeta)$, we realize that for $|\zeta| < |\zeta_c|$ and large values of k_c, this function does not depend on k_c and the approximation

$$\lim_{k_c \to \infty} \widetilde{\Phi}_{k_c} = \widetilde{\Phi}(\zeta)$$

is used to define the true scaling function $\widetilde{\Phi}(\zeta)$ of the scaling variable ζ. This fact was already hypothesized in the scaling theory of conduction in disordered systems [9, 11, 12]. We show here in addition that true scaling is valid only up to the crossover point $|\zeta_c|$ where

$$\frac{\tilde{d}}{2}\frac{\pi}{\sin(\pi u)}|\zeta_c|^u \approx k_c^{t/D\nu}. \tag{41}$$

The true scaling function $\widetilde{\Phi}(\zeta)$ is a complex function of the complex variable ζ; therefore its graphical representation is somewhat complex, as is shown in figure 3.

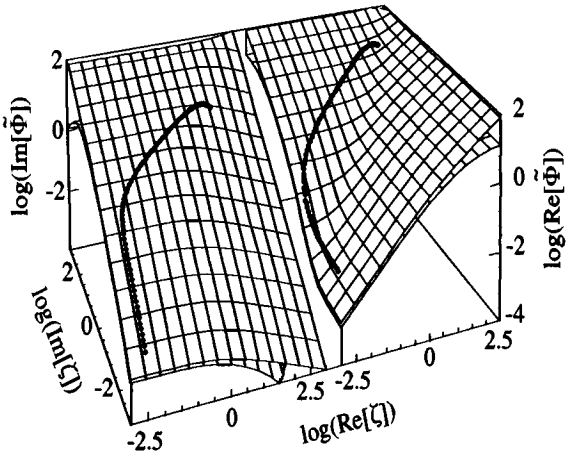

Figure 3. Surfaces representing the real and imaginary parts of the scaling function $\widetilde{\Phi}$ as a function of the real and imaginary part of the scaling variable ζ for $k_c = \infty$ (top surface) and $k_c = 25$ (bottom surface). Points show experimental data ($\phi = 28$ and $T = 25\ ^\circ$C) from [22].

It represents in a three-dimensional plot the real and imaginary parts of $\widetilde{\Phi}(\zeta)$ as functions of the real and imaginary parts of ζ. It clearly shows the linear, power-law and constant regions of the scaling function; a typical set of conductivity and permittivity data for the WAD system [22] are also reported in order to relate the experiments to the theory. Figure 4 shows the k-dependence of $\sigma(\omega)$ for typical values of the parameters. The left-hand part shows $\epsilon''(\omega)$, to highlight the progressive shift to lower frequencies of the relaxation process, on approaching percolation. Note also the progressive increase in intensity. The right-hand part of the figure shows the $\sigma(\omega)$-data on a log–log scale to highlight the initial Debye-like increase, followed by a power-law region in ω^u. The width in frequency of the power-law region increases on approaching percolation.

4.2. The percolation threshold

At the percolation threshold, where $k_c \to \infty$, $\widetilde{\sigma}(\omega)$ can be evaluated as

$$\widetilde{\sigma}(\omega) = \Sigma_u \widetilde{\sigma}_B \frac{D\nu}{t}\, {}_2F_1\left(1, u; 1+u; -\frac{1}{B_1\tilde{h}}\right) \tag{42}$$

where ${}_2F_1$ is a Gauss hypergeometric function defined by the relation

$$\int_1^\infty \mathrm{d}x\ \frac{x^a}{1+zx^b} = \frac{1}{z(b-a-1)}\, {}_2F_1\left(1, \frac{b-a-1}{b}; 1+\frac{b-a-1}{b}; -\frac{1}{z}\right). \tag{43}$$

From the previous equations one can calculate the static conductivity and permittivity at percolation for $\omega = 0$, i.e. using $\tilde{h} = \sigma_A/\sigma_B$. For intermediate frequencies

$$\widetilde{\sigma}(\omega) \approx \Sigma_u \widetilde{\sigma}_B \frac{\tilde{d}}{2} \frac{\pi}{\sin(\pi u)} \left(\frac{1-\omega_A\tau_1}{1-\omega_A\tau}\frac{\omega_B\tau - 1}{\omega_B\tau_1 - 1}\right)^u \tag{44}$$

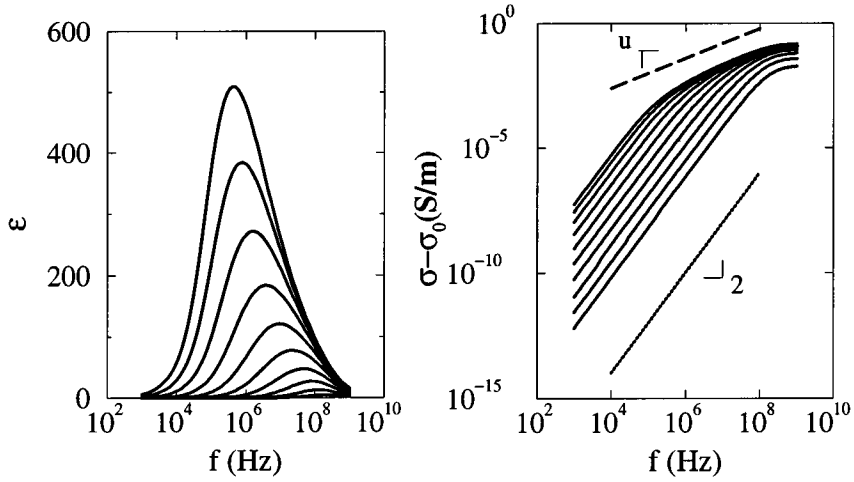

Figure 4. $\epsilon''(\omega)$ and $\sigma(\omega)$ for different values of k ($k = 2^n$, with $n = 1, 10$). The same data are shown on a linear scale, as the imaginary part of the dielectric constant, on the left, and on a log–log scale on the right. The two lines are power laws with exponent 2 (Debye) and exponent u. The parameters are the same as for figure 1.

which in the RC case becomes

$$\tilde{\sigma}(\omega) \approx \Sigma_u \sigma_B \frac{\tilde{d}}{2} \frac{\pi}{\sin(\pi u)} (\mathrm{i}\omega\tau_1)^u \tag{45}$$

and shows the typical power-law behaviour in frequency of both the conductivity and the permittivity.

4.3. The relation to the Cole–Davidson formula

We can define the susceptibility $\tilde{\chi}$ of the microemulsion through the relation

$$\epsilon_\infty \tilde{\chi}(\omega) = \int_1^\infty \mathrm{d}k\ c(k)\epsilon_{k\infty}\tilde{\chi}_k(\omega) = \int_1^\infty \mathrm{d}k\ c(k) \frac{\epsilon_A \Delta_k}{1 + \mathrm{i}\omega\tau_k} \tag{46}$$

that, using the cluster relaxation time as an integration variable, can be evaluated as

$$\frac{\tilde{\chi}(\omega)}{\tilde{\chi}(0)} = \frac{1}{\mathcal{N}} \int_{\tau_1}^{\omega_A^{-1}} \frac{\mathrm{d}\tau}{\tau} \left(\frac{1 - \omega_A\tau_1}{1 - \omega_A\tau} \right)^{-u} \left(\frac{\omega_B\tau - 1}{\omega_B\tau_1 - 1} \right)^{1-u} \times \exp\left[-\frac{1}{k_c} \left(\frac{1 - \omega_A\tau_1}{1 - \omega_A\tau} \frac{\omega_B\tau - 1}{\omega_B\tau_1 - 1} \right)^{\tilde{d}/2} \right] \frac{1}{1 + \mathrm{i}\omega\tau} \tag{47}$$

where the normalization $\mathcal{N}$ is given by the same integral for $\omega = 0$. We can write the rather complex expression of (47) in a simple fashion in the RC limit:

$$\frac{\tilde{\chi}(\omega)}{\tilde{\chi}(0)} = \frac{1}{\mathcal{N}} \int_{\tau_1}^\infty \frac{\mathrm{d}\tau}{\tau} \left(\frac{\tau}{\tau_1} \right)^{1-u} \exp\left[-\left(\frac{\tau}{\tau_c} \right)^{\tilde{d}/2} \right] \frac{1}{1 + \mathrm{i}\omega\tau} \tag{48}$$

where τ_c, the relaxation time corresponding to the cut-off cluster size k_c, is for the RC case

$$\tau_c = \tau_1 k_c^{2/\tilde{d}}.$$

This expression for $\tilde{\chi}(\omega)$ is close to the well-known empirical Cole–Davidson relaxation time distribution. In fact, in that case too, the relaxation time distribution is given by a power law with a cut-off, substituted for in our case with an exponential function playing the same role.

5. The time correlation function

The susceptibility $\tilde{\chi}$ of the microemulsion, according to linear response theory, is related to the Laplace transform of the time derivative of the polarization time correlation function

$$\begin{aligned}\epsilon_\infty \tilde{\chi}(\omega) &= -\int_0^\infty \mathrm{d}t\ \mathrm{e}^{-\mathrm{i}\omega t}\frac{\mathrm{d}}{\mathrm{d}t}\left[\frac{V}{k_B T}\langle\mu(t)\mu(0)\rangle\right] \\ &= -\int_0^\infty \mathrm{d}t\ \mathrm{e}^{-\mathrm{i}\omega t}\frac{\mathrm{d}}{\mathrm{d}t}\left[\int_1^\infty \mathrm{d}k\ c(k)\epsilon_A\Delta_k \mathrm{e}^{-t/\tau_k}\right] \end{aligned} \tag{49}$$

from which we can derive the normalized polarization time correlation function $C(t)$:

$$C(t) = \frac{\langle\mu(t)\mu(0)\rangle}{\langle\mu^2(0)\rangle} = \frac{1}{\mathcal{N}}\int_1^\infty \mathrm{d}k\ c(k)\Delta_k \mathrm{e}^{-t/\tau_k} \tag{50}$$

where the normalization $\mathcal{N}$ is given by the same integral with $t = 0$. Data on complex conductivity can then be transformed from frequency to time to give the normalized correlation function. $C(t)$ can also be written as the average of an exponential decay over a relaxation time distribution:

$$\begin{aligned}C(t) = \frac{1}{\mathcal{N}}\int_{\tau_1}^{\omega_A^{-1}} \frac{\mathrm{d}\tau}{\tau}\left(\frac{1-\omega_A\tau_1}{1-\omega_A\tau}\right)^{-u}\left(\frac{\omega_B\tau-1}{\omega_B\tau_1-1}\right)^{1-u} \\ \times\ \exp\left[-\frac{1}{k_c}\left(\frac{1-\omega_A\tau_1}{1-\omega_A\tau}\frac{\omega_B\tau-1}{\omega_B\tau_1-1}\right)^{\tilde{d}/2} - \frac{t}{\tau}\right].\end{aligned} \tag{51}$$

In this case too we recover a simple expression in the RC limit:

$$C(t) = \frac{1}{\mathcal{N}}\int_{\tau_1}^\infty \frac{\mathrm{d}\tau}{\tau}\left(\frac{\tau}{\tau_1}\right)^{1-u}\exp\left[-\left(\frac{\tau}{\tau_c}\right)^{\tilde{d}/2} - \frac{t}{\tau}\right] \tag{52}$$

the behaviour of which we examine in detail in the various time regions. We start by evaluating $C(t)$ for short times, where

$$C(t) \approx 1 - \frac{\tilde{d}/2u}{\Gamma(2(1-u)/\tilde{d})}\left(\frac{\tau_1}{\tau_c}\right)^{1-u}\frac{t}{\tau_1} \tag{53}$$

which is valid for $t \ll \tau_1$, while for $t \gg \tau_1$

$$C(t) \approx 1 - \frac{\tilde{d}}{2u(1-u)}\frac{\Gamma(1+u)}{\Gamma(2(1-u)/\tilde{d})}\left(\frac{t}{\tau_c}\right)^{1-u} \tag{54}$$

valid up to $t \ll \tau_c$, the longest cluster relaxation time. For $t \gg \tau_c$ we find a stretched exponential decay:

$$C(t) \approx \exp\left[-\left(\frac{t}{\beta'(1-\beta')^{1/\beta'-1}\tau_c}\right)^{\beta'}\right] \tag{55}$$

where the universal exponent β' is related only to $\tilde{d}$:

$$\beta' = \frac{\tilde{d}}{\tilde{d}+2}. \tag{56}$$

To summarize, the time behaviour of the time correlation function of dipole fluctuations $C(t)$ is dominated by two time-scales τ_1 and τ_c given by the monomer and largest cluster relaxation time respectively. As shown in the left-hand part of figure 5, $C(t)$ starts for short times as an exponential and evolves to a power-law behaviour for long times. Finally, as shown in the right-hand part of figure 5, $C(t)$ behaves like a stretched exponential. Note also that the size of the intermediate power-law region increases on approaching percolation. It is interesting to note that a similar behaviour is experimentally observed in glassy systems and predicted in part by mode-coupling theories [23].

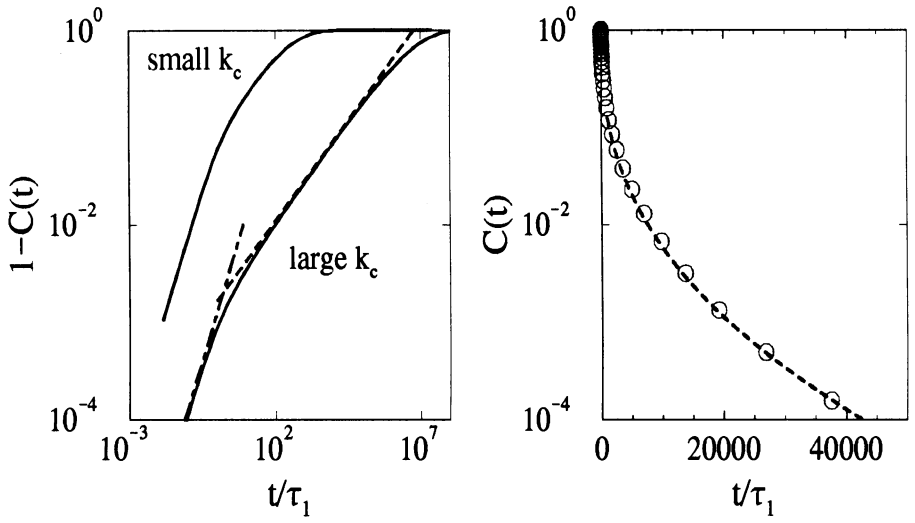

Figure 5. The normalized polarization correlation function $C(t)$ as a function of time. In this case $\tau_1 = 400$ ps. The left-hand panel shows $1 - C(t)$ in order to highlight the initial exponential decay and the intermediate power law. The right-hand part shows the long-time stretched exponential behaviour. Circles show the experimental data of [22].

6. Comparison with the experimental results

In this section we will mainly deal with multicomponent microemulsions, the phase diagram of which has been studied in great detail. We will refer in particular to the WAD system that has been analysed in a series of investigations [2, 3, 7, 24]. The phase diagram at constant molar ratio $X = [\text{water}]/[\text{AOT}] = 40.8$ is characterized by a region of coexistence of liquid microemulsion droplet phases bound by the binodal line and a critical point at $\phi \approx 0.1$ and $T \approx 40\ ^\circ$C. A percolation line extends from very low volume fractions, close to the critical point, up to very high volume fractions $\phi \approx 0.8$ [24].

Before describing the comparison with the experimental results, we briefly discuss how one can describe the phase diagram of the system. This situation can be modelled in terms of a simple liquid-state theory via interacting spheres. In fact, the existence of a critical point is an indication of the presence of an attractive interaction between the microemulsion droplets. The interaction potential can be modelled in various ways, e.g. as a hard-sphere repulsion and an attractive potential well [25, 26]. A particularly simple model stems from the limiting case of a potential well, the range of which tends to zero, while its depth

becomes increasingly negative. In this case a thermodynamic state is described by the interaction strength and the system volume fraction. The model is then exactly soluble in the Percus–Yevick approximation of the Ornstein–Zernike equation, as shown by Baxter [25]. The attractive feature of this model, beyond the fact that it is analytically soluble and capable therefore of giving in particular the coexistence curve and the critical point, is the possibility of deriving from it the percolation locus as the set of points where the average cluster size diverges [27]. The percolation line evaluated from the Baxter model [28] reproduces in a rather good quantitative way the experimentally measured one [29].

In order to compare the experimental data with the theoretical predictions, we need to introduce a mapping between the variables of the model and the physical parameters of the microemulsion. In particular, we need to know the relationship between k_c and $|T - T_P|$ or $|\phi - \phi_P|$. In model bond percolation, the connectivity length ξ_P depends on the bond probability p and is characterized, close to the threshold p_P, by the power law

$$\xi_P = \xi_0 |p - p_P|^{-\nu} \tag{57}$$

with amplitude ξ_0 and exponent ν. On the other hand we can define ξ_P as

$$\xi_P = R_1 k_c^{1/D}. \tag{58}$$

By comparison of (58) and (57) we derive the relation between the cut-off cluster size and the distance from percolation:

$$k_c = \left(\frac{\xi_0}{R_1}\right)^D |p - p_P|^{-\nu D} \tag{59}$$

which implies in our model that $\sigma_0 \approx |p - p_P|^{s'}$. By postulating a linear dependence of $|p - p_P|$ on $|T - T_P|$ we get $\sigma_0 \approx |T - T_P|^{s'}$. Such linear dependence is consistent with an analytic relation between p and T.

Figure 6 shows the experimentally measured static conductivity as a function of temperature for a WAD system in which water has been substituted for with brine (see [30]). The solid curve is the theoretical expression of equation (32). Note that at T_P, σ_0 reaches a finite value, related to the finite conductivity of the oil phase. Thus the power-law behaviour $\sigma_0 \approx |T - T_P|^{s'}$ can be observed only in a finite T-window, not too close to T_P.

We now turn to the frequency dependence of the complex conductivity. Figure 7 compares $\sigma(\omega)$ and $\epsilon(\omega)$ for some data for microemulsion systems close to percolation taken from the literature [2, 3, 7] with the theoretical expression of (32). Figure 8 compares theory and experiment for $\epsilon'(\omega)$ and $\epsilon''(\omega)$ for two different volume fractions of the WAD system close to the percolation line [22]. Figure 9 shows a set of values of $\sigma(\omega)$ on approaching percolation by increasing temperature.

In all cases, the conductivity $\tilde{\sigma}(\omega)$ describes very well, and with the same set of parameters simultaneously, the ω-dependence of σ and ϵ of the samples, as well as their limiting zero- and infinite-frequency values. It depends on the five parameters ω_A, ω_B, τ_1, Σ_u and k_c. We find $\omega_A \approx 0.1$–0.5 MHz and $\omega_B \approx 2$–4 GHz for all systems, and $\tau_1 \approx 100$–500 ps. The k_c-values obtained from the fit increase monotonically on approaching the transition, going from a few droplets far from percolation, to about 10^4 close to it. The parameters τ_1 and σ_u can also be related to the amplitude and the characteristic time of the monomer relaxation, which in turn are connected to the electrical parameters of the materials. We stress that these fitting parameters are the minimal set that one can use to describe completely at a quantitative level the dielectric behaviour of a two-component system.

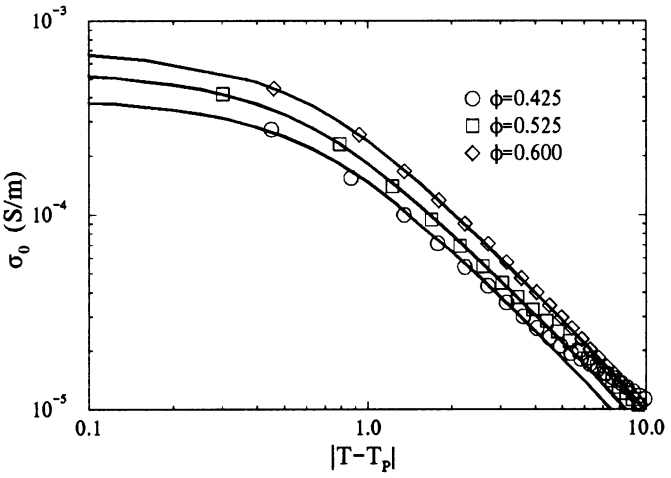

Figure 6. Static conductivity as a function of $T - T_P$ for three different volume fractions of a brine–AOT–decane system [30]. Solid lines show the theoretical expressions (32).

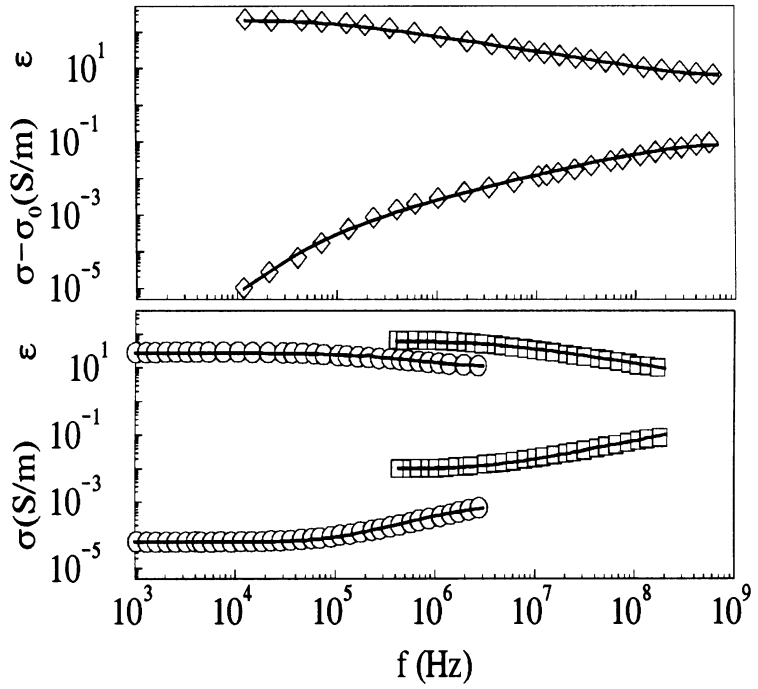

Figure 7. The complex conductivity in WAD systems. The data were taken from (◯) [3], (□) [7], (◇) [2]. Solid lines show the theoretical expressions (32).

7. Summary and conclusions

Water-in-oil microemulsions, in the phase where an ionic surfactant separates water droplets from the surrounding oil bath, constitute one of the few liquid systems where a percolation

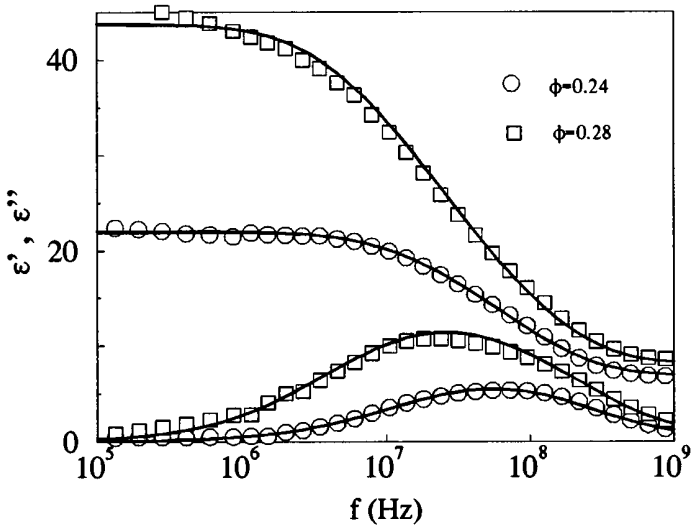

Figure 8. Real and complex permittivity in WAD systems [22], for two different volume fractions approaching percolation. Solid lines show the theoretical expressions (32).

line can be clearly defined experimentally. Electrical conductivity measurements at low frequencies can be used to define a percolation line in a plane of temperature and dispersed phase composition. Percolation phenomena are in a sense defined by the type of probe used to detect them, e.g. for electrical percolation one defines touching droplets as the basic units of the clusters. It is well known that instead along the electrical percolation line the scattered light intensity does not show any anomaly. Indeed the compressibility diverges only at the critical point and along the spinodal line.

Once the percolation line for electrical conductivity is defined, one can phenomenologically parametrize the conductivity and permittivity in terms of power laws, which provide evidence of the scaling character of the phenomenon. Power laws characterize the dynamic conductivity and dielectric constant too, with relaxation frequencies generally in the MHz region. More generally a complete scaling behaviour, expressed as power laws and associated scaling functions, is obtained for the behaviour of the complex conductivity.

In order to introduce a quantitative description of the anomalous electric behaviour due to percolation below the threshold, we use a simple model where dynamic percolation is the key ingredient. We assume that the charge carriers present, due to the ionic nature of the surfactant, perform an anomalous diffusive motion in the bulk of the fractal clusters formed by aggregation of the initial microemulsion droplets, and determine in this way the relaxation amplitude and time of a single cluster. In order to do this analytically, we use an effective-medium approximation which gives the corrected dependence of the cluster conductivity on the electrical material parameters. The use of the scaling cluster size distribution, to take into account the polydispersity of the microemulsion, gives the final formula of our model.

We derive from the model frequency-dependent complex electrical conductivities that are in very good quantitative agreement with measurements performed by many authors on various systems. The distance from the percolation line in T of ϕ is measured by the cut-off of the cluster size distribution k_c. We also derive the full scaling behaviour of the complex

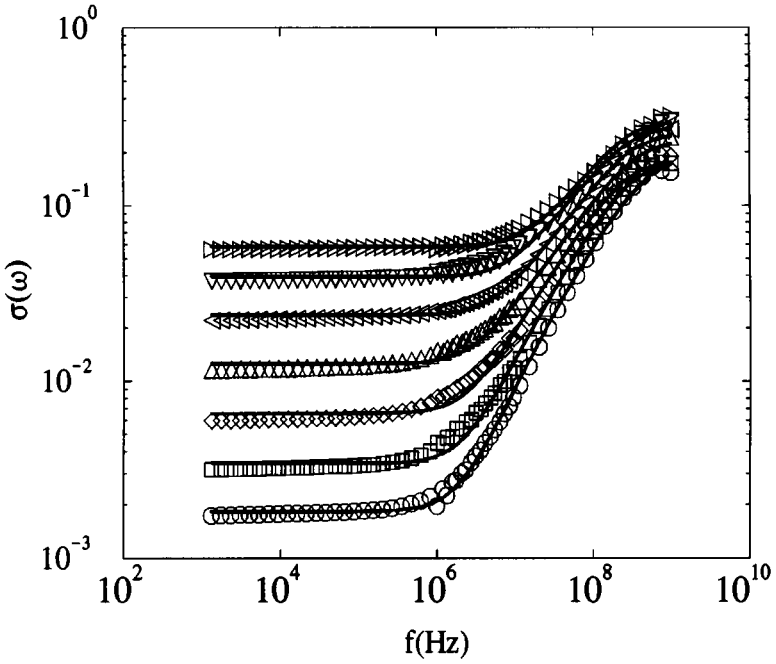

Figure 9. The frequency dependence of the conductivity in a WAD system as a function of temperature on approaching percolation. From bottom to top, the temperatures goes from 19 °C to 24 °C. Solid lines show the theoretical expressions (32).

conductivity. From the latter we calculate via Laplace transformation the time correlation function $C(t)$ of the polarization fluctations, i.e. the quantity that one could measure with experiments in the time domain, via time domain reflectometry for instance. It is worth emphasizing the evolution in time of $C(t)$, which is very similar to that encountered for glassy systems. After an initial exponential decay it shows a power law in time and then evolves to a stretched exponential for very long times, with a universal exponent connected to the spectral dimension. We finally determine the crossover times between the various behaviours. They are essentially the relaxation times τ_1 for the initial monomers, typically of the order of a few hundred nanoseconds, and τ_c for the largest cluster present in the microemulsion, which diverges at the percolation threshold where the infinite clusters form.

Acknowledgments

Most of this work is the result of a long-standing collaboration with Sow-Hsin Chen over several years. We are indebted to him for introducing us to the field of complex liquids and for enlightening scientific suggestions and discussions. The research of F Bordi, C Cametti, F Sciortino and P Tartaglia is supported by GNSM/CNR and INFM/MURST.

References

[1] Lagües M, Ober R and Taupin C 1978 *J. Physique Lett.* **39** L487
[2] van Dijk M A 1985 *Phys. Rev. Lett.* **55** 1003

[3] Bhattacharya S, Stokes J P, Kim M W and Huang J S 1985 *Phys. Rev. Lett.* **55** 1884
[4] Boned C, Peyrelasse J and Saidi Z 1993 *Phys. Rev.* E **47** 468
[5] Clarkson M T and Smedley 1988 *Phys. Rev.* A **37** 2070
Clarkson M T 1988 *Phys. Rev.* A **37** 2079
[6] Cametti C, Codastefano P, Tartaglia P, Rouch J and Chen S H 1990 *Phys. Rev. Lett.* **64** 1461
[7] Ponton A, Bose T K and Delbos G 1991 *J. Chem. Phys.* **94** 6879
[8] Feldman Y, Kozlovich N, Nir I and Garti N 1995 *Phys. Rev.* E **51** 478
[9] Clerc J P, Giraud G, Laugier J M and Luck J M 1990 *Adv. Phys.* **39** 191 and references therein
[10] Lagües M 1979 *J. Physique Lett.* **40** L331
[11] Grest G S, Webman I, Safran S and Bug A L R 1986 *Phys. Rev.* A **33** 2842
[12] Gefen Y, Aharony A and Alexander S 1983 *Phys. Rev. Lett.* **50** 77
[13] Cametti C, Sciortino F, Tartaglia P, Rouch J and Chen S H 1995 *Phys. Rev. Lett.* **75** 569
[14] Bruggemann D A G 1935 *Ann. Phys., Lpz.* **24** 636
[15] Rouch J, Tartaglia P and Chen S H 1993 *Phys. Rev. Lett.* **71** 1947
[16] Coniglio A and Klein W 1980 *J. Phys. A: Math. Gen.* **13** 2775
[17] Berthier S 1988 *Ann. Phys., Paris* **13** 503 and references therein
[18] Hanai T 1968 *Emulsion Science* ed P Sherman (New York: Academic)
[19] In [13] the same symbol, Δ_k, was used for the monomer contribution to the relaxation amplitude.
[20] Stauffer D and Aharony A 1992 *Introduction to Percolation Theory* (London: Taylor and Francis)
[21] The argument of the exponential in (19) should be $-(k/k_c)^{2\sigma}$, with the index σ given by 0.45 in three dimensions [20]. We assume $2\sigma \approx 1$ in order to be able to write analytical formulae.
[22] Cametti C, Codastefano P, Di Biasio A, Tartaglia P and Chen S H 1989 *Phys. Rev.* A **40** 1962
[23] See
Transport theory and statistical physics 1995 *Supercooled Liquids* **24** 1149 (Issue devoted to relaxation kinetics (S Yip, Guest Editor)
[24] Chen S H, Rouch J, Sciortino F and Tartaglia P 1994 *J. Phys.: Condens. Matter* **6** 10855
[25] Baxter R J 1968 *J. Chem. Phys.* **49** 2770
[26] Kranendonk W G and Frenkel D 1988 *Mol. Phys.* **64** 403
[27] Coniglio A, De Angelis U and Forlani A 1977 *J. Phys. A: Math. Gen.* **10** 1123
[28] Chiew Y C and Glandt E D 1983 *J. Phys. A: Math. Gen.* **16** 2599
[29] Chen S H, Ku C Y, Rouch J and Tartaglia P 1995 *Int. J. Thermodyn.* **16** 1119
[30] Bordi F, Cametti C, Codastefano P, Sciortino F, Tartaglia P and Rouch J 1996 *Prog. Colloid Polym. Sci.* at press